COBEM 2021 26th International Congress of Mechanical Engineering
November 22-26, 2021, Virtual Congress, Brazil
ABCM Associação Brasileira de Engenharia e Ciências Mecânicas

COB-2021-2105
CHARACTERISTIC LENGTHS OF LIQUID PROPELLANT ROCKET ENGINES AND THE INFLUENCE OF CHEMICAL REACTIONS

Maurício Sá Gontijo
Department of Aerospace Engineering, University of Brasília UnB, St. Leste Projeção A - Gama Leste Brasília - DF 72444-240, Brazil
mauricio.sa.gontijo@gmail.com

Gustavo Alexandre Achilles Fischer
Federal Institute of Education, Science and Technology of Santa Catarina - IFSC, Rodovia, SC-443, 845 - Vila Rica, Criciúma - SC, 88813-600, Brazil
gustavo.fischer@ifsc.edu.br

Fernando de Souza Costa
Combustion and Propulsion Laboratory - LABCP, National Institute for Space Research - INPE, Rodovia Presidente Dutra, km 40, 12630-000, Cachoeira Paulista / SP - Brazil
fernando.costa@inpe.br

Abstract. *The characteristic length (L^*) is an extremely important parameter on the design of liquid propellant rocket engines (LPREs) and it is being studied in several works through many years. In addition, the atomization plays a fundamental role on the prediction of the L^* and it can be measured by the Sauter Mean Diameter (SMD). Also, chemical reactions may have a considerable influence on the results of these predictions. It is proposed in this work an algorithm that evaluates the SMD effects and the influence of chemical reactions on the characteristic length with a low computational cost, providing a powerful tool for propulsion engineers. Additionally, the algorithm was validated with real consecrated engines using three propellant mixtures, the ethanol/liquid oxygen, RP-1/liquid oxygen and liquid hydrogen/liquid oxygen, on a range of 20 to 260 bar of chamber pressure. In addition, a comparison of L^* for these propellant mixtures was conducted simulating the L75 rocket engine. The results showed that the increase of the L^*, when it is not considered that chemical reactions occurs in a infinitesimal length, varies from approximately 1.5% to 20.3%, with an average of 8.42% and that there is an average value of equivalence ratio required to reach the minimum L^* in function of the propellant mixture.*

Keywords: *Characteristic Lengths, Sauter Mean Diameters, Chemical Reactions, Liquid Propellant Rocket Engines*

1. INTRODUCTION

On the design process of liquid propellant rocket engines, one of the most important propulsive parameters is the characteristic length. This parameter is responsible to provide enough volume for the complete injection, atomization, mixing and combustion of the propellants in the combustion chamber. Analyzing the L^* is substantial, due to in case of a larger chamber than necessary, losses due to heat transfer and weight becomes too large. In case of a smaller chamber than necessary, incomplete combustion is reached and combustion instabilities may occur (Huzel and Huang, 1992), (Humble *et al.*, 1995).

A previous work was focused on ethanol/LOx and RP-1/LOx, which stands for Rocket Propellant 1 and liquid oxygen, respectively, and validated the proposed algorithm using engines such as the V-2, L75 and F-1 engines as a comparison Gontijo *et al.* (2020). The present work will be focused on studying cryogenic propellants, such as LOx and LH_2, which is liquid hydrogen, used in various engines and it is used in extremely low temperatures. Some of these engines were the RS-25, from the space shuttle, and RL10A-3-3A. This type of propellants started to be used in a experimental way since 1945 for launch vehicles upper stages. The first engine that flew using cryogenic propellants was Pratt Whitney RL 10 (Sutton, 2006), (Sutton, 2003). The chamber pressure of rocket engines that uses cryogenic propellants varies between 30 to 227.5 bar (Sutton, 2006), (Hugh, 1995). However, the Raptor engine, from SpaceX, can reach a chamber pressure of 330 bar, using LOx and LCH_4, which is liquid methane. Brazil still doesn't work with a full cryogenic engine, although L5, L15 and L75 does uses LOx as oxidizer (Gontijo *et al.*, 2020). The use of LH_2 is very complex, specially due to embrittlement of the tank structure in consequence of the low temperatures (around 15 K). Considering these information, this work presents an analysis of engines that has a range of chamber pressure varying from 20 to 260 bar using LH_2/LOx, RP-1/LOx and ethanol/LOx.

2. LITERATURE REVIEW

A mathematical definition of the L^* is given by:

$$L^* = \frac{V_c}{A_t} \tag{1}$$

where V_c is the chamber volume and A_t is the throat area. Tabulated data presented on many references such as (Huzel and Huang, 1992) and (Humble *et al.*, 1995) can't provide information on how characteristic length varies with chamber pressure and mixture ratio.

Droplet vaporization models are frequently used for more accurate results. (Turns, 2012) present two simple vaporization models, the first one is vaporization without combustion and the second is considering combustion of the droplet. In addition, a third model is presented considering a one-dimensional vaporization-controlled combustion, which is more close to what happens in rocket engines, however it is not accurate as others available models. A work made by (Priem and Heidmann, 1960) is able to predict the combustion efficiency based on droplet vaporization. Some other works even implemented turbulence intensity influence on the vaporization (Khan *et al.*, 2018). More complex models are presented by (Wang, 2016), that can consider an evaporation of a group of droplets, sub-critical evaporation and other characteristics, and by (Salvador, 2004), that can consider droplets thermal expansion and droplets deformation due to drag.

Spalding's model is one of the most used models to predict the L^* due to its low computational costs, since it is a uni-dimensional model, and due to accurate results. The equation below presents the L^* equation proposed by Spalding (Spalding, 1958), (Spalding, 1959).

$$L^* = \xi^* {r_0}^2 \left[\frac{2}{\gamma+1} \left(\frac{G}{\rho\sqrt{\gamma R T_C}} \right)^2 \frac{\gamma-1}{\gamma+1} \right]^{\frac{\gamma+1}{2(\gamma-1)}} \frac{c_p \rho_L}{k} \frac{\sqrt{\gamma R T_C}}{ln\,(1+B)} \tag{2}$$

where ξ^* is a dimensionless minimum chamber length and it is calculated by Eq. (3), r_0 is the injected droplet radius, γ is the specific heat ratio, G is the propellant mass flux, ρ is the density of the combustion products, R is the gas constant, T_C is the adiabatic flame temperature, c_p is the specific heat at constant pressure of the combustion products and B is the transfer number, shown in Eq. (5).

$$\xi^* = \frac{\chi_0 + 0,3S}{2+S} \tag{3}$$

where $\chi_0 = u_0/u_g$, u_0 is velocity at injection, u_g is gas final velocity in combustion chamber and S is droplet drag, derived from Stoke's law, calculated below:

$$S = \frac{9 c_p \mu/k}{2B} \tag{4}$$

where μ is the dynamic viscosity.

$$B = \frac{H \cdot m_o}{Q \cdot r} + c_{p,L} \frac{T_g - T_s}{Q} \tag{5}$$

where H is a fuel calorific value, m_o is the weight concentration of oxygen, Q is vaporization enthalpy, r is the weight of oxygen required for combustion of unit weight fuel, $c_{p,L}$ is the specific heat at constant pressure on liquid phase (if using liquid propellant), T_g is gas stream temperature, and T_s is the temperature of the surface engaging in mass transfer (boiling temperature). Other formulations of the transfer number are explained by (Spalding, 1958) and (Gontijo *et al.*, 2020).

An analysis made in a previous work was made with equations shown above and it was possible to conclude that the injector design has more than 60% of impact on L^*, in which 58% is due to SMD, which is a parameter that represents the injected droplet diameter. However, this analysis was made considering that chemical reactions occurs in a infinitesimal length (Gontijo *et al.*, 2020).

In addition, the last work defined a new propulsive parameter, which was the ϕ^*, that is called as characteristic equivalence ratio and represents the equivalence ratio required to reach a minimum characteristic length. It was found that the alteration of the ϕ^* is small with varying the chamber pressure, also it is mainly dependent on propellant mixture and it can be modeled by logarithmic functions for a wide range of chamber pressure.

Using Equation (3) it is not possible to account the extra length required for the chemical reactions to occur. In this way, an improvement of the algorithm used on (Gontijo *et al.*, 2020) is required, even though it is quite precise.

3. THEORETICAL MODEL

The analytical equation shown in Eq. (2) was derived by (Spalding, 1959) assuming that the chemical loading tends to zero and that chemical reactions occur in an infinitesimal length. With this assumption, the temperature along the combustion chamber is uniform and equal to gas temperature in chemical equilibrium and combustion happens when the radius of the droplet is infinitesimal. In practical cases this condition doesn't occur, since temperature varies along the combustion chamber, the temperature of the gas is not in chemical equilibrium, due to changes in chemical composition of combustion products across the internal flow, and an additional length for combustion (chemical reactions) is necessary. This means that it is fundamental to evaluate chemical reactions influence on the droplet vaporization during the rocket engine operation (Adler, 1959).

Pressure swirl injectors were considered in this work due to the fact that most of the engines studied uses this type of injector. To calculate SMD, the Radcliffe model (Lefebvre and McDonell, 2007) was used and it is described below:

$$SMD = 7,3\sigma^{0,6}{v_L}^{0,2}\dot{m}_L^{0,25}\Delta P^{-0,4} \tag{6}$$

where σ is the surface tension, v_L is the kinematic viscosity, $\dot{m}_L$ is the liquid mass flow rate and ΔP is the pressure drop in the injector. This SMD model, from Radcliffe (Lefebvre and McDonell, 2007), was used since it presented accurate results in predicting the size of the injected droplets by pressure swirl injectors (Gontijo *et al.*, 2020), (Fischer, 2019).

The vaporization model proposed by (Adler, 1959) uses dimensionless equations for the droplet velocity, radius and temperature, and for the gas velocity, as stated by (Spalding, 1959). Since the dimensionless distance variable does not occur explicitly in those equations, it may be eliminated by combining them. And the η relation, which is the fractional decrease in the droplet radius, facilitate the integration and it is calculated by:

$$\eta = \frac{r_0 - r}{r} = 1 - \zeta = 1 - \frac{r}{r_0} \tag{7}$$

where r is the droplet radius at any adjacent position, r_0 is SMD/2 and ζ is the dimensionless droplet radius. When $\zeta = 0$ the dimensionless distance, obtained by integrating the differential equation of $d\zeta/d\xi$, is equal to ξ^*.

According to (Adler, 1959), the dimensionless differential equation of the droplet velocity is calculated by the following equation:

$$\frac{d\chi}{d\eta} = \frac{S}{(1-\eta)\,\tau}\left[\eta\left(\eta^2 - 3\eta + 3\right) - \chi\right] \tag{8}$$

where $\chi = u(\xi)/u_g$, which u is function of the dimensionless length ξ, and τ is a dimensionless temperature or reactedness.

According to (Adler, 1959), the dimensionless differential equation of τ is calculated by:

$$\frac{d\tau}{d\eta} = \frac{(1-\eta)}{\eta\left(\eta^2 - 3\eta + 3\right)}\left[\frac{\psi}{L\tau}\chi - 3\,(1-\eta)\,\tau\right] \tag{9}$$

where L is a chemical loading and ψ is a dimensionless reaction rate function, which is practically only function of τ, calculated by:

$$\psi\,(\tau) = (n+1)\left(1 + \frac{1}{n}\right)^n (1-\tau)\,\tau^n \tag{10}$$

where n is an integer that modifies the form of the reaction rate.

Since the chemical reaction influence is being taken in consideration, the chemical loading, which is a function of χ, ψ, η and τ, don't tends to zero anymore, as stated in (Spalding, 1959), and can be calculated using the equation below:

$$L = \frac{\chi_0 \cdot \psi\,(\tau_0)}{3{\tau_0}^2} \tag{11}$$

The Equation (11) was derived assuming that $\frac{d\tau}{d(1-\eta)} = 0$, since for majority size of the droplet this is a reasonable approximation (Adler, 1959). The value of L varies from 0 and a critical value L_c, which is obtained by combining Eqs. (10) and (11) and it is calculated with the following equation.

$$L_c = \frac{\chi_0}{3}\left(\frac{n+1}{n-1}\right)\left(1 + \frac{1}{n}\right)^n \left(1 + \frac{1}{n-1}\right)^{n-2} \tag{12}$$

The ratio of L_c/χ_0 in function of n gives the information that combustion is possible or not. In that case, if $L/\chi_0 < L_c/\chi_0$ the combustion is possible and the algorithm must consider chemical reactions.

Finally, ξ^*, which is substituted in Eq. (2), is calculated with the following equation:

$$\xi^* = \int_0^1 \frac{\chi}{\tau} \zeta \, d\zeta \tag{13}$$

The boundary conditions for Equation (13) are:

$$\zeta = 0 \quad ; \quad \chi = 1 \quad ; \quad u = u_g \quad ; \quad \tau = \tau_1 \leq 1 \tag{14}$$

In order to calculate the chemical reactions between the propellants and thermodynamic and gas dynamic properties, the software CEA (Chemical Equilibrium with Applications) (Gordon and McBride, 1994) was used. To solve Equations (8) and (9), a Runge-Kutta (4,5) numerical method was used and it ends when η reaches 1, or $\zeta = 0$. However, the first step of the numerical solution needs to be calculated analytically with:

$$\chi_1 = \chi_0 + \left(\frac{d\chi}{d\eta}\right)_0 h \tag{15}$$

$$\tau_1 = \tau_0 + \left(\frac{d\tau}{d\eta}\right)_0 h = \tau_0 + \left[\frac{(s-\tau_0)(1-\tau_0)}{(n-2)(1-\tau_0)-1}\right] h \tag{16}$$

where h is an integration step size and it is defined as $h = -\eta + 1$. The boundary conditions for Equations (15) and (16) are:

$$\eta = 0 \quad ; \quad \chi = \chi_0 = u_0/u_g \quad ; \quad \tau = \tau_0 \tag{17}$$

Also, an approximate solution is proposed by (Adler, 1959). The approximate solution is an analytical solution that may be used in order to decrease computational costs in case of being implemented on large algorithms for optimization of a whole LPRE, for example. However, it is not as accurate as the numerical solution.

By analyzing the chemical reactions of consecrated propellant mixtures, such as LH_2/LOx, RP-1/LOx and ethanol/LOx, it is possible to predict that the influence of chemical reactions on characteristic length will be larger on mixtures with more complex products. With this statement, it is expected that the mixture LH_2/LOx will have a lowest impact by the combustion.

It is also perceptible by the transfer number (Eq. (5)) that LH_2/LOx mixture tends to have lower characteristic length, since the boiling temperature (T_s) is much lower than the other fuels (20 K). Other parameters can be evaluated analyzing Tab. 3.

4. ROCKET ENGINES AND ITS PARAMETERS

More engines than the ones analyzed at (Gontijo *et al.*, 2020) will be studied in this work to provide a more solid validation of the algorithm and it is even possible to make some statistical analysis. The engines and its parameters are show in Tabs. 1 and 2.

Table 1: Combustion chamber parameters (Hugh, 1995), (Gontijo *et al.*, 2020).

Engine	**Propellant**	P_c **[Mpa]**	L^* **[m]**	A_c/A_t	D_c **[m]**
HM7B	LH_2/LOx	3.6	0.68	2.78	0.18
RL10A-3-3A	LH_2/LOx	3.2	0.95	2.95	0.262
HM60	LH_2/LOx	10	0.84	2.99	0.415
J-2	LH_2/LOx	5.4	0.62	1.58	0.47
LE-7	LH_2/LOx	12.7	0.78	2.75	0.4
SSME	LH_2/LOx	20.5	0.8	2.96	0.45
F-1	RP-1/LOx	7.76	1.22	1.17	1.02
V-2	Hydrated ethanol/LOx	1.5	2.87	5.31	0.922
L75 - old	RP-1/LOx	6	1.57	5.49	0.211
L75	Hydrated ethanol/LOx	6	1.27	3.67	0.088

Table 2: Injection parameters (Hugh, 1995), (Gontijo *et al.*, 2020), (Astrium, 2012), (Pouliquen, 1984), (Stapp, 2016), (NASA, 1968), (Boeing, 1998), (Bilstein, 1996).

Engine	ΔP **[kPa]**	$\dot{m}_L$ **[kg/s]**	$\dot{m}_p$ **[kg/s]**	**No. Fuel Injectors**	**Injector type**
HM7B	920	2.26	13.9	90	swirl coaxial
RL10A-3-3A	558	2.8	16.8	216	swirl coaxial
HM60	800*	34	232	516	swirl coaxial
J-2	683	36.1	242.3	614	swirl coaxial
LE-7	1038	35.2	246.3	452	swirl coaxial
SSME	1200	67	469	600	swirl coaxial
F-1	641	742	2526	1404	impinging
V-2	234	58	130	1224	various
L75 - old	619.68*	6.4	22	91	swirl coaxial
L75	619.68*	8.85	22.95	91	swirl coaxial

*ΔP relation (Kessaev, 1997) shown in Eq. (18)

where P_c is the chamber pressure, A_c/A_t is contraction ratio shown in Eq. (19), D_c is chamber diameter, and $\dot{m}_p$ is the propellant mass flow rate. ΔP for the last two engines and HM60 weren't available, so it was used a relation presented by (Kessaev, 1997), shown below:

$$\Delta P = 80\sqrt{10P_c} \tag{18}$$

where P_c is given in pascals.

$$A_c/A_t = \frac{1}{M_c}\sqrt{\left[\frac{1+\left(\frac{\gamma-1}{2}\right)M_c{}^2}{1+\left(\frac{\gamma-1}{2}\right)}\right]^{\frac{\gamma+1}{\gamma-1}}} \tag{19}$$

where M_c is the Mach number at the end of the combustion chamber and calculated using the finite chamber area method of CEA, and it is defined below:

$$M_c = \frac{u_g}{a} = \frac{u_g}{\sqrt{\gamma R T_c}} \tag{20}$$

where a is the speed of sound, $R = R_0/M$, where R_0 is the universal gas constant ($R_0 = 8.31446$ J/(molK)) and M is the molecular weight of the combustion gas products.

The fuels properties are displayed on Table 3. These properties were taken at 298.15 K for anhydrous ethanol and RP-1, and 18.95 K for LH_2 and at 1 atm.

Table 3: Injection parameters (NIST, 2021), (Keesom and Macwood, 1938).

Properties	**Anhydrous ethanol**	**RP-1**	**LH_2**
σ [N/m]	0.0236	0.0280	0.00218
c_{pL} [J/gK]	2.57	2.29	9.56
v_L [m²/s]	$1.402{\cdot}10^{-6}$	$1.867{\cdot}10^{-6}$	$19.76{\cdot}10^{-6}$
Q [J/kg]	841719.12	348413.23	510560
H [MJ/kg]	28.2	45	142
ρ_L [kg/m³]	788.3	799.1	72.49
T_s [K]	20	450	351.5

5. RESULTS AND DISCUSSIONS

Running the algorithm for the engines shown in Tables 1 and 2 with data from Tab. 3, the results were obtained considering chemical reactions influence and $n = 4$. Those results are displayed in Tabçe 4.

Table 4: Comparison between real L^* with the results considering and not considering chemical reactions influence

Engine	**Real L^* [m]**	**L^* without chemical reactions influence [m]**	**L^* with chemical reactions influence† [m]**	**Increase of L^* [%]**
HM7B	0.68	0.69	0.72	4.35
RL10A-3-3A	0.95	0.62	0.65	4.84
HM60	0.84	1.27	1.31	3.15
J-2	0.62	0.84	0.98	16.67
LE-7	0.78	1.20	1.15	4.17
SSME	0.8	1.34	1.36	1.49
F-1	1.22	1.17	1.35	13.33
V-2	2.87	2.02	2.43	20.29
L75 - old	1.57	1.32	1.48	12.12
L75	1.27	1.33	1.38	3.76

†For $n = 4$

According to these results it is possible to understand how characteristic length is influenced by those parameters shown in Tabs. 1, 2 and 4. Most of these influences were discussed by (Gontijo *et al.*, 2020), who proposed which parts on engine design must be focused to decrease the required characteristic length. Some of these relations are that SMD, G and T_s must be the lowest and P_c must be the highest. In addition, the evaluation of the impact of chemical reactions with the mathematical model discussed on Section 3.was made and compared with results without the extra length for chemical reactions in Tab. 4. Last column of Table 4 shows that, in average, the increase in L^* is of about 8.42% comparing with and without chemical reactions additional length. Some results gave an increase of more than 10% on L^*, this shows that chemical reactions space cannot be neglected. Some differences between real and calculated characteristic lengths are visible on Table 4, those differences may be explained by some reasons listed below:

1. Not all of these engines used pressure swirl injectors, such as F-1;
2. Some of these engines used various injectors, besides the pressure swirl type, such as V-2;
3. Engines that used ethanol as fuel, didn't use anhydrous ethanol;
4. Engines that used RP-1 as fuel may have used different degrees of refinement, which is common;
5. It was considered an uniform mixture ratio, however many of these engines used different mixture ratios along its radius;
6. Film cooling can influence on L^* and it was not considered in this work;
7. Break-up mechanisms and collision of sprays wasn't considered;
8. One-dimensional models don't consider tri-dimensional trajectories;
9. Turbulence effects are neglected;
10. Lastly, not all engines were designed with minimum L^*.

According to the items listed above, it is comprehensible that there is differences between real L^* and calculated ones, with and without chemical reactions influence. Nonetheless, the most important information is how much L^* increases with the addition of the chemical reactions influence and those are valuable data to decide either to implement or not this model. It is clear analyzing Table 4 that it is essential to model this phenomenon.

Contour plots in Figure 1 shows results of the characteristic length without chemical reactions influence, using Eqs. (2) and (3), in function of the chamber pressure and the equivalence ratio, ϕ, which is highly used in propellant mixtures studies and analysis of rocket engines. Equivalence ratio is a parameter to express the mixture ratio between the propellants and is defined bellow:

$$\phi = \frac{F/O}{(F/O)_{st}} = \frac{\dot{m}_f/\dot{m}_{ox}}{(\dot{m}_f/\dot{m}_{ox})_{st}} \tag{21}$$

where $\dot{m}_f$ is the fuel mass flow rate, $\dot{m}_{ox}$ is the oxidizer mass flow rate and the subscript st means that it is on the stoichiometric condition.

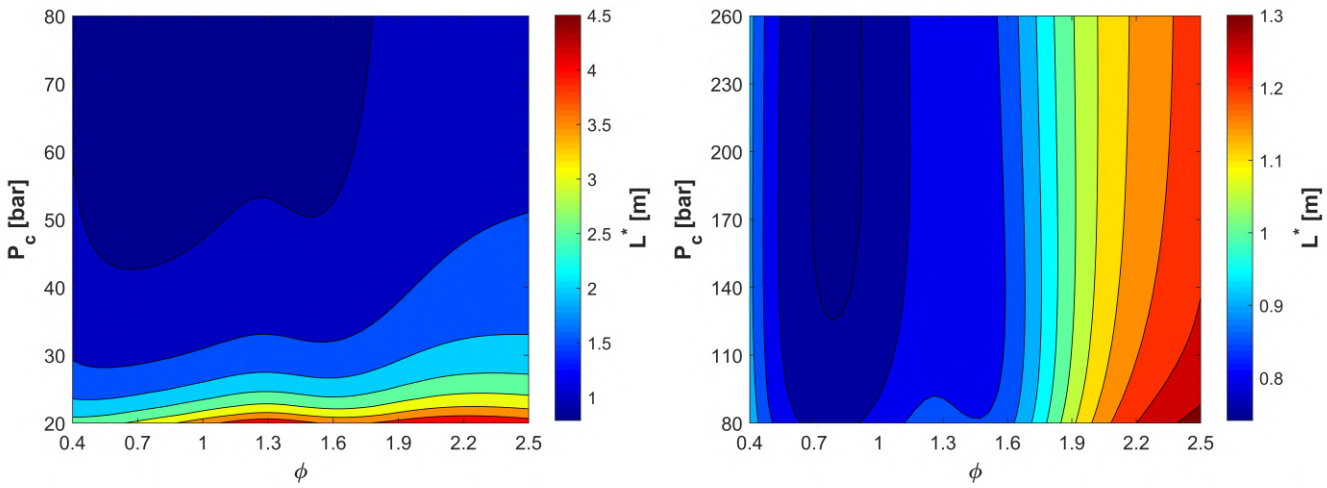

Figure 1: L^* for ethanol/LOx without chemical reactions influence under a) low P_c and b) high P_c

Analyzing graphs plotted in Figure 1, a region of convergence is visible, in which the optimum L^* is reached. This region is easily identified by a dark blue contour. This is more perceptible when using high chamber pressures. The optimum ϕ will be better discussed on Figure 5, that shows the equivalence ratio required to reach that region.

Now, in order to obtain results for the three propellant mixtures studied in this work, Fig. 2 represents the influence of the equivalence ratio and chamber pressure on characteristic length of ethanol/LOx, Fig. 3 for RP-1/LOx and Fig. 4 for LH_2/LOx. In addition, a comparison between Figures 1 and 2 can be made and it is possible to understand how much the chemical reactions impact on the results. There was an increase of about 0.25 m on the minimum value of characteristic length, in which represents an impact of 33,33%. For the case of ethanol and liquid oxygen propellant mixture, an optimum region is reached with an equivalence ratio between 0.7 and 0.9 and with the higher P_c as possible.

In addition, as already said, the higher is the chamber pressure, the lower is the characteristic length. This is one of the main reasons that companies wants to reach the maximum P_c as possible. Also, the engine performance increases, which is a highly desirable characteristic.

Another remark is that the mixture ratio required for the minimum L^* is almost the same, this means that ϕ^* has low dependence on chemical reactions influence.

For the simulations with chemical reactions influence, using n = 1 is a conservative approximation, since it means that $L_c \to \infty$, then combustion is always possible ($L/\chi_0 < L_c/\chi_0$, from Eq. (12)). Also, high values of n are used for more complex molecules, so n = 4 is a reasonable value for the propellant combinations used in this work.

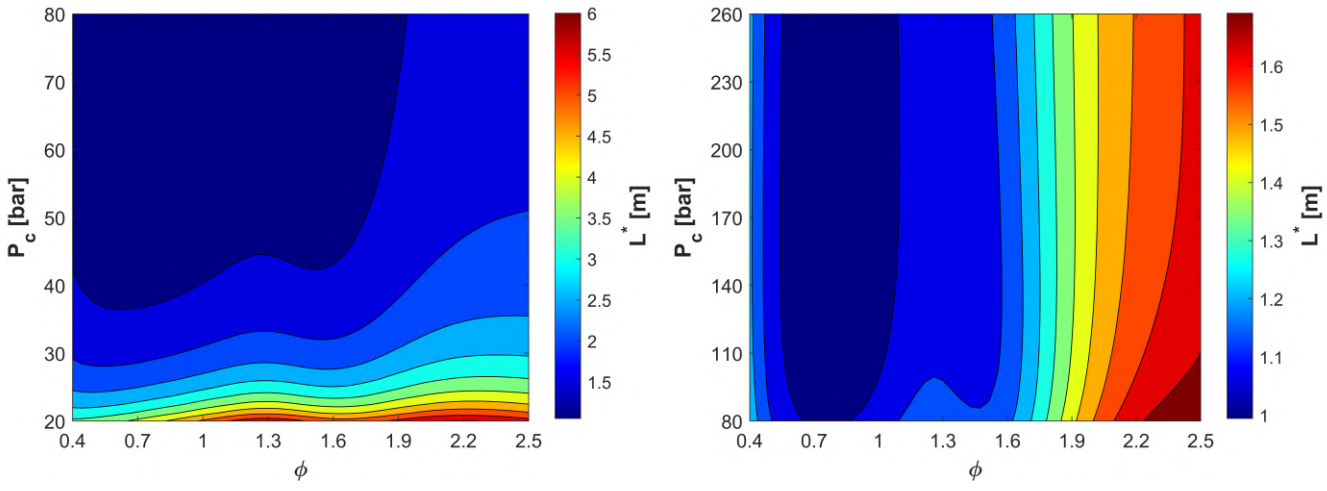

Figure 2: L^* for ethanol/LOx under a) low P_c and b) high P_c with chemical reactions influence (n = 4)

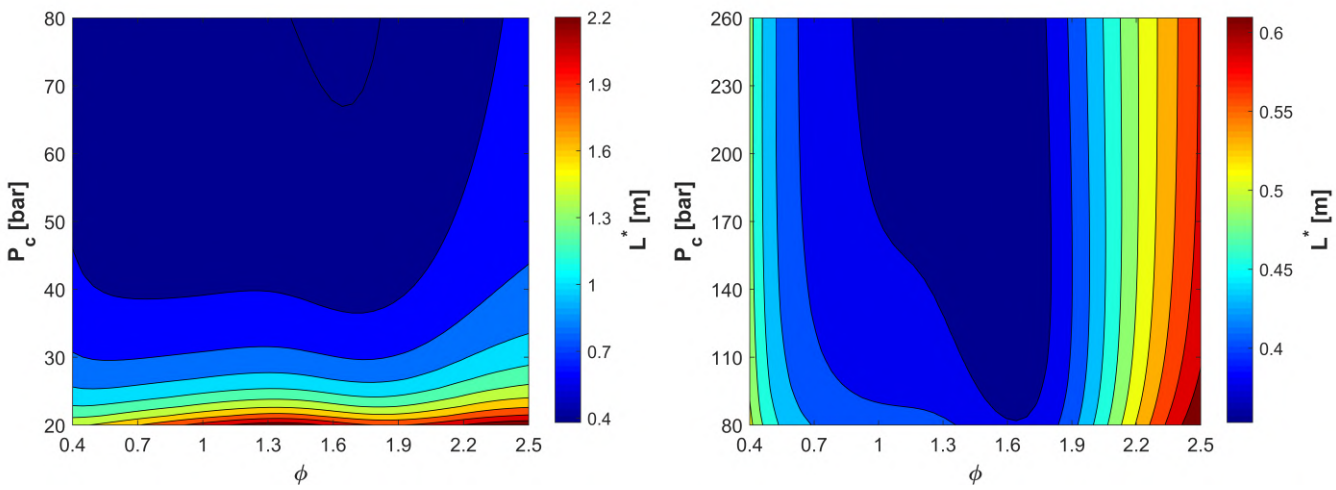

(a) (b)

Figure 3: L^* for RP-1/LOx under a) low P_c and b) high P_c with chemical reactions influence (n = 4)

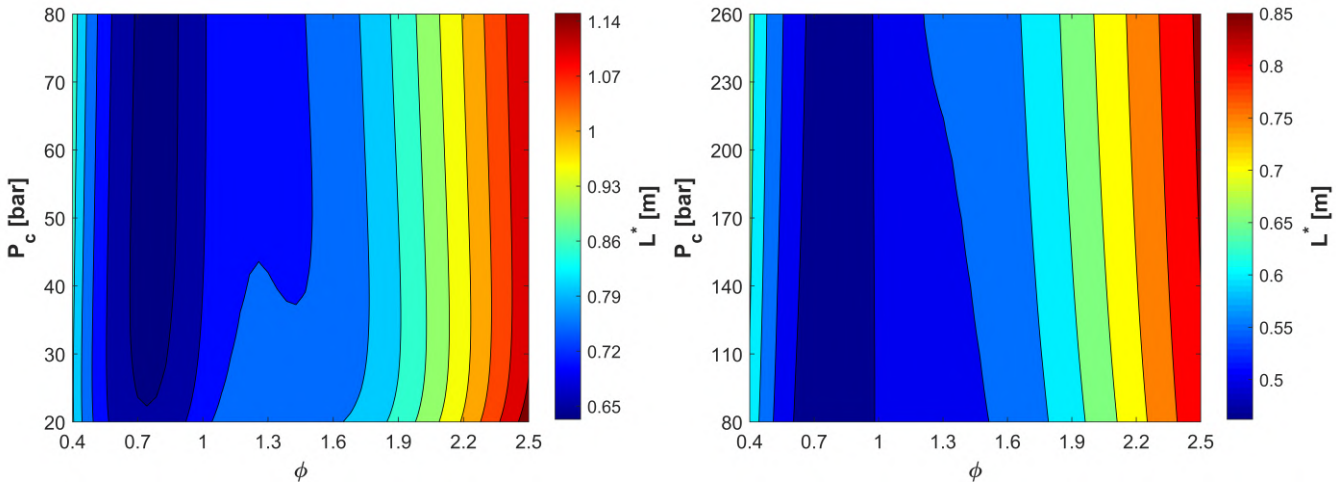

(a) (b)

Figure 4: L^* for LH_2/LOx under a) low P_c and b) high P_c with chemical reactions influence (n = 4)

The analysis made above was made using the same engine (L75) with identical parameters, only propellant mixture was changed. These parameters were 8.85 kg/s of fuel mass flow rate in 91 pressure swirl injectors, 14.10 kg/s of oxidizer mass flow rate, chamber and throat radius of 0.044 and 0.023 m, respectively, 3.67 of contraction ratio and pressure drop and chamber pressure of 6.19 and 60 bar, respectively (Gontijo *et al.*, 2020).

As seen in Figure 4, LH_2/LOx presented the lowest required L^*, in comparison with Figs. 2 and 3. This happened, mainly, because its adiabatic flame temperature is the highest, the fuel boiling temperature is the lowest and surface tension is the lowest.

In addition, other simulations were performed with n = 1, 2, 4 and 8 to verify the impact of this parameter on the results. An obtained average increase in L^*, for the LPREs of Tab. 4, was of about 19.37%, 14.82%, 8.42% and 7.98%, respectively. However, as discussed previously, for the propellant mixtures considered in this work, $n = 4$ is a reasonable value. For LH_2/LOx a smaller value, such as $n = 2$, could be used, since molecules are simpler than alcohols and hydrocarbons.

The equivalence ratio required to reach the minimum characteristic length, ϕ^* Gontijo *et al.* (2020), for the three propellant mixtures varying with P_c is shown on graph of Fig. 5.

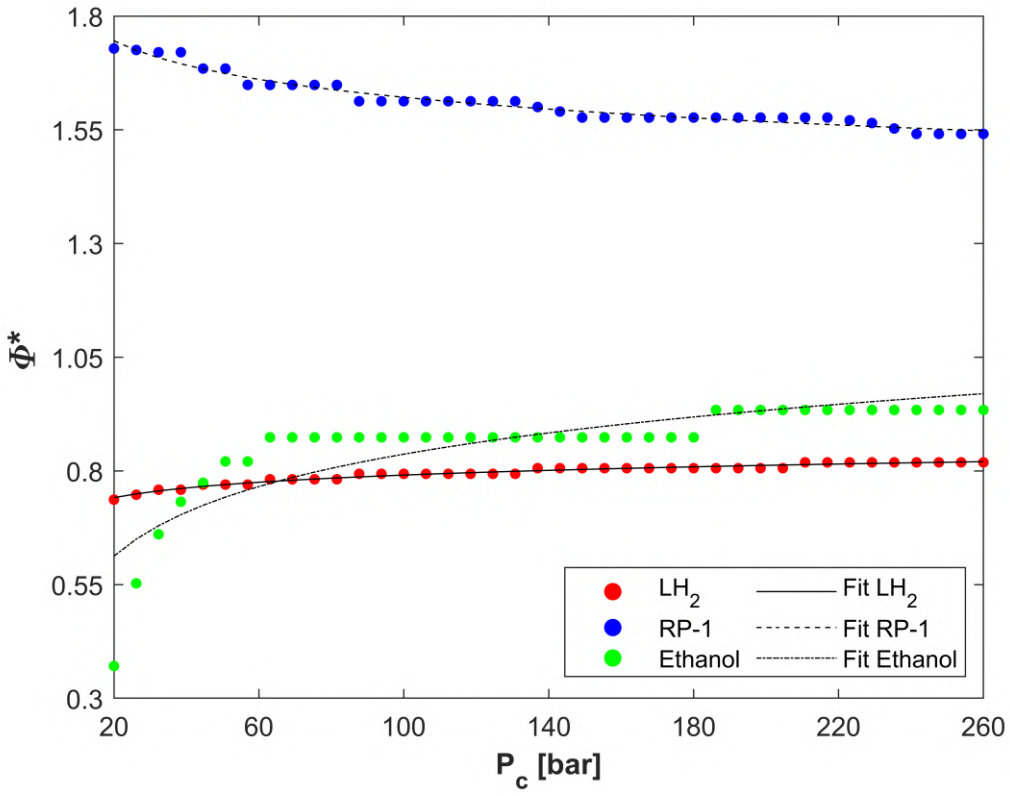

Figure 5: ϕ^*, for RP-1/LOx, ethanol/LOx and, LH_2/LOx varying with P_c

Figure 5 shows that ϕ^* has an average value of 0.859, 1.594 and 0.796 for ethanol/LOx, RP-1/LOx and, LH_2/LOx, respectively, and can be calculated with simple polynomial functions shown in Eq. (22), for LH_2/LOx, Eq. (23), for RP-1/LOx, and Eq. (24), for ethanol/LOx. These values of are compatible with several engines, such as F-1, S-4(MA-3), H-1, RS-27, L75 and others (Hugh, 1995), (Gontijo *et al.*, 2020). Neglecting chemical reactions influence, the values were 0.779, 1.632 and 0.748, respectively (Gontijo *et al.*, 2020).

$$LH_2: \quad \phi^* = 0.031\ln(P_c) + 0.649 \quad ; \quad R^2 = 0,986 \tag{22}$$

$$RP{-}1: \quad \phi^* = -0.077\ln(P_c) + 1.976 \quad ; \quad R^2 = 0,981 \tag{23}$$

$$Ethanol: \quad \phi^* = 0.139\ln(P_c) + 0.1956 \quad ; \quad R^2 = 0,853 \tag{24}$$

Equations above allows to predict accurately, and in a fast way, the ϕ^*. These are promising relations, capable of providing the equivalence ratio, or mixture ratio, to reach the minimum characteristic length in function of the chamber pressure.

6. CONCLUSIONS

In this work is presented an algorithm that considers chemical reactions effect on the characteristic length prediction. In addition, the algorithm created has low computational costs (taking few seconds to calculate) and it is a useful and simple tool capable of providing an accurate approximation of the L^*, reducing the amount of required numerical simulations and experimental testing, which tends to be massively more costly.

By analyzing several engines, it was concluded that the chemical reactions plays a role of increasing the characteristic length from 1.5% to 20.3%, and about 8.42% in average. In case of some engines, such as L75, SSME, HM7B, RL10A-3-3A and LE-7, this increase is less than 5%. However, on engines like F-1, V-2, J-2 and SSME, the values are higher than 10%. A 10% of augmentation on the L^* is considerable and proves that chemical reactions additional length cannot be neglected.

In addition, a contribution to the ϕ^* was given in this work, by updating the results obtained previously by adding the chemical reactions contributions and by including the LH_2/LOx propellant mixture. These information are helpful in pre-design phases, were the engineer can make a close selection of the equivalence ratio to be used, in order to reach a minimum characteristic length in function of P_c. For RP-1/LOx, ethanol/LOx and LH_2/LOx the obtained values of ϕ^* were 0.796, 1.594 and 0.859, respectively.

7. REFERENCES

Adler, J., 1959. "A one-dimensional theory of liquid-fuel rocket combustion. part ii. the influence of chemical reaction". *Imperial College of Science and Technology, London*.

Astrium, 2012. "Hm-7 and hm-7b rocket engine - thrust chamber". Astrium, https://web.archive.org/web/20120508062948/http://cs.astrium.eads.net/sp/launcher-propulsion/rocket-engines/hm7b-rocket-engine.html. Accessed 10 April 2021.

Bilstein, R.E., 1996. "Stages of saturn". *NASA*.

Boeing, 1998. "Space shuttle main engine orientation". *Rocketdyne Propulsion and Power*.

Fischer, G.A.A., 2019. "Atomização de géis por injetores centrífugos duais e jato-centrífugos para aplicação em propulsão de foguetes". *Doctorate thesis on Space Engineering and Technology/Combustion and Propulsion - INPE*.

Gontijo, M.S., Fischer, G.A.A. and Costa, F.S., 2020. "Evaluation of smd effects on characteristic lengths of liquid rocket engines using ethanol/lox and rp-1/lox". 18^{th} *Brazilian Congress of Thermal Sciences and Engineering*.

Gordon, S. and McBride, B.J., 1994. "Computer program for calculation of complex chemical equilibrium compositions and applications i. analysis". *NASA, Reference Publication 1311*.

Hugh, B.M., 1995. "Numerical analysis of existing liquid rocket engines as a design process starter". *31st, AIAA/ASME/SAE/ASEE Joint Propulsion Conference, July, San Diego, CA*.

Humble, R.W., Henry, G.N. and Larson, W.J., 1995. *Space Propulsion Analysis and Design*. McGraw-Hill.

Huzel, D.K. and Huang, D.H., 1992. *Modern Engineering for Design of Liquid-Propellant Rocket Engines*. American Institute of Aeronautics and Astronautics.

Keesom, W.H. and Macwood, G.E., 1938. "The viscosity of liquid hydrogen". *Physica V, no 8, 745-748*.

Kessaev, J.V., 1997. "Theory and calculation of liquid-propellant engines". *Moscow Aviation Institute*.

Khan, T., Qamar, I., Shah, F., Akhtar, K. and Akhtar, R., 2018. "Model for fuel droplet evaporation in combustion chamber of liquid propellant rocket engines". *Journal of Engineering and Applied Sciences, Vol. 37, No. 1*.

Lefebvre, A.H. and McDonell, V.G., 2007. "Atomization and sprays". *CRC Press, 2ª Ed.*

NASA, 1968. "J-2 engine". *NASA, Saturn V News Refference*.

NIST, 2021. "Nist chemistry webbook". National Institute of Standards and Technology, https://webbook.nist.gov/chemistry/. Accessed 10 April 2021.

Pouliquen, M.F., 1984. "Hm60 cryogenic rocket engine for future european launchers". *Journal of Spacecrafts and Rockets, Vol. 21, No. 4, pp. 346-353*.

Priem, R.J. and Heidmann, M.F., 1960. "Propellant vaporization as a design criterion for rocket engine combustion chambers". *NASA TR-67*.

Salvador, C.A.V., 2004. "Modelo matemático de câmaras de combustão bipropelentes". *Masters dissertation on Space Engineering and Technology/Combustion and Propulsion - INPE*.

Spalding, D.B., 1958. "Combustion in liquid-fuel rocket motors". *Imperial College of Science and Technology, London*.

Spalding, D.B., 1959. "A one-dimensional theory of liquid-fuel rocket combustion". *Imperial College of Science and Technology, London*.

Stapp, D.T., 2016. "An investigation of the performance potential of a liquid oxygen expander cycle rocket engine". *Master of Science. University of Alabama*.

Sutton, G.P., 2003. "History of liquid propellant rocket engines in the united states". *Journal of Propulsion and Power, Vol. 19, No. 6*.

Sutton, G.P., 2006. "History of liquid propellant rocket engines". *AIAA*.

Turns, S.R., 2012. "An introduction to combustion: Concetps and applications". *McGraw Hill, 3rd Ed.*

Wang, Z.G., 2016. "Internal combustion process of liquid rocket engines: Modeling and numerical simulations". *Wiley, 1st Ed.*

8. RESPONSIBILITY NOTICE

The authors are solely responsible for the printed material included in this paper.